

# Experimental Studies of Combustor Dilution Zone Aerodynamics, Part I: Mean Flowfields

S. J. Stevens\* and J. F. Carrotte†

*University of Technology, Loughborough, England, United Kingdom*

An experimental investigation has been carried out to study circumferential irregularities in the temperature distribution downstream of a row of 16 heated jets injected normally into a confined annular crossflow at a momentum flux ratio of 4. The heated air was fed to the plunged holes along a representative approach annulus and, despite the uniformity of the approach flow, the velocity profile across the exit plane of each dilution hole revealed a complex flowfield that varied in a random manner from one jet to another. Temperature distributions measured at a plane two hole diameters downstream indicated a lack of symmetry between the dilution jets because of an apparent twist of the temperature contours associated with certain jets. Velocity distributions at the same location indicated a corresponding asymmetry in the double-vortex structure formed in the wake of each jet.

## Nomenclature

$D$	= diameter of dilution holes
$J$	= momentum flux ratio ( $= \rho_j V_j^2 / \rho_c V_c^2$ )
$R_p$	= radius of plunging on dilution holes
$r$	= radius
$r_i$	= inner radius of crossflow annulus
$r_n$	= nondimensional radius [ $= (r - r_i) / (r_o - r_i)$ ]
$r_o$	= outer radius of crossflow annulus
$S$	= distance between dilution holes
$T$	= temperature
$T_b$	= block temperature
$T_c$	= reference crossflow temperature
$T_j$	= reference jet temperature
$T_r$	= area-weighted mean temperature at radius $r$
$(T_b)_r$	= block temperature at radius $r$
$U, V, W$	= velocities in $X, Y, Z$ directions
$V_c$	= velocity of crossflow
$V_j$	= absolute velocity of jet
$X$	= coordinate measured from hole center in downstream direction
$Y$	= coordinate measured normal to injection wall in radial direction
$Z$	= coordinate measured from hole center in a lateral direction
$\alpha$	= pitch angle of jet measured from radial ( $Y$ ) axis
$\gamma$	= jet asymmetry parameter
$\theta$	= nondimensional temperature [ $= (T - T_c) / (T_j - T_c)$ ]

## Superscripts

$(\hat{a})$	= maximum
$(\bar{A})$	= mean

## Introduction

THE flowfield associated with a row of round jets injected normally into a confined crossflow has been the subject of intensive investigation for many years,<sup>1-9</sup> since it has important practical implications in the mixing process occurring in gas turbine combustors and in the cooling of turbine blades. This investigation is concerned with the mixing process occurring in the dilution zone of combustors, where patterns of jets dilute the hot gases leaving the combustor and are therefore a major factor in determining the outlet temperature distribution. The desired temperature profile is determined mainly by stress and corrosion considerations in the first-stage nozzle guide vanes and rotor blades, and the degree to which the desired profile can be obtained determines the life of the turbine at the required operating conditions.

A comprehensive study of the mixing of air jets injected into a rectangular duct has been conducted by Holdeman and co-workers,<sup>4,7-9</sup> in which jet diameter and spacing, mixing duct geometry, and velocity and temperature ratios were varied. It was concluded that the most important parameter influencing the mixing process is the jet-to-crossflow momentum flux ratio, this being confirmed independently by the results of Sridhara<sup>2</sup> when investigating the mixing of air jets injected into a circular duct. Although much of the experimental work has been conducted with jets injected from one side toward an opposite wall, it has been shown by Holdeman et al.<sup>7</sup> and Kamotani and Greber<sup>3</sup> that this wall may be regarded as a plane of symmetry and that results should apply equally well to combustors with directly opposed dilution jets. However for this to be true it is important that the velocities of the two opposing jets be closely matched and that allowance should be made for the enhanced rate of mixing due to the change in effective mixing duct geometry.

The continuing pressure to improve engine performance dictates the use of higher compressor delivery pressures and combustor exit temperatures, both of which reduce the required combustor volume. However, any attempt to achieve the smaller volume by reducing the length of the dilution zone usually leads to a lowering in the quality of the outlet temperature distribution. In this respect the occurrence of local "hotspots" or circumferential asymmetries is particularly important, since they effectively limit the mean combustor exit gas temperature and therefore reduce the engine per-

Presented as Paper 87-1827 at the AIAA/SAE/ASME/ASEE 23rd Joint Propulsion Conference, San Diego, CA, June 29-July 2, 1987; received Sept. 23, 1988; revision received Feb. 15, 1989. Copyright © 1987 American Institute of Aeronautics and Astronautics, Inc. All rights reserved.

\*Professor, Aeronautical Propulsion.

†Research Assistant, Department of Transport Technology.

formance and turbine blade life. Such asymmetries often occur in a random manner and vary in magnitude and position with different combustors built to the same design. It has been suggested that one of the main sources of such asymmetries is irregularities within the primary zone. However, even in experiments with carefully controlled primary zone exit conditions, the effect has persisted,<sup>10</sup> leading to the suspicion that these asymmetries are created within the dilution zone. Some of this may be because of jet impingement on other jets that have insufficient directional bias, or a lack of symmetry between the dilution jets. Unfortunately, with the exception of that due to Crabb and Whitelaw,<sup>5</sup> all of the published work has concentrated on the radial distribution of temperature, and as yet no satisfactory explanation has been given for this important phenomenon.

In this experimental program attention has been focused on the relationship between the behavior of dilution jets and the mechanisms causing asymmetry, rather than on a parametric investigation of the relative significance of the large number of aerodynamic and geometric variables involved in defining the dilution process. The experiments were carried out on a fully annular facility incorporating single-sided dilution, and particular care was taken to insure that the feed to the dilution holes passed along a representative approach annulus. All dilution measurements were performed at a jet-to-crossflow momentum flux ratio of 4, with upstream feed and crossflow annulus velocities of approximately 7 and 14.7 m/s, respectively.

### Characteristics of Jets in a Crossflow

As each jet of fluid issues from a dilution hole it creates a blockage in the crossflow, and as a consequence the flow immediately ahead of the jet decelerates, causing an increase in pressure. Downstream a rarefaction occurs and this, combined with the increased upstream pressure, provides a force that deforms the jet. Because of the intensive mixing of the jet with the crossflow, a turbulent shear layer rapidly develops around the periphery of the jet and reduces the size of the potential core. The lower momentum fluid in the shear layer at the sides of the jet will, under the influence of the pressure forces, take on a more curved trajectory than that of the higher-velocity fluid in the core (Fig. 1). This gives rise to the formation of the characteristic "kidney"-shaped jet profile downstream of the holes. This effect is enhanced by the more-curved trajectory of the lower-momentum fluid at the front of the jet, which is forced to accelerate around the sides of the higher-velocity core fluid before rolling up into two "core" vortices located at the lobes of the jet. Furthermore, in the case of multiple jets issuing into a confined crossflow two vortices (hereafter referred to as crossflow vortices) are formed by crossflow fluid that passes between the jets into the low-pressure region sited in their wake. Close to the wall the fluid moves in a predominantly lateral direction with very little axial momentum, and as it penetrates inward from either side it moves upward away from the wall until further movement is

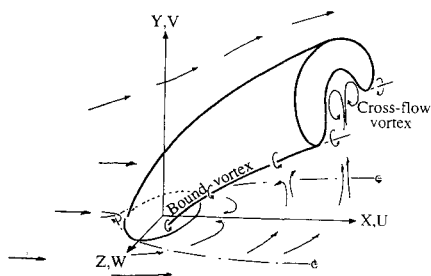


Fig. 1 Multiple jets in a crossflow.

prevented by the presence of the jet. The flow then rolls up to form two crossflow vortices located beneath the core of the jet. The action of these vortices augments the entrainment of fluid, causing large-scale mixing with the jet.

### Test Facility

The test facility, illustrated in Fig. 2, is comprised of three vertically mounted, concentric Plexiglas tubes, the space between the inner and center casing forming the dilution hole feed annulus of 35.8-mm height and the space between the center and outer casing forming the crossflow annulus of 76.2-mm height. Air is drawn from the atmosphere by a centrifugal fan into the crossflow annulus via a plenum chamber, a bell-shaped inlet flare, and a honeycomb flow straightener. A heater mounted on top of the plenum chamber is supplied from a second fan that draws air from the laboratory. The heated air (55°C) then passes via a pipe and an annular nozzle into the dilution hole feed annulus. Supplying heat in this way gives information on the dispersal of jet fluid as well as identifying the trajectory of the high-temperature core. In addition, by mounting the facility in the vertical plane the influence of buoyancy on the penetration of the jets is eliminated.

The array of dilution jets is formed by 16 equispaced, 25.4-mm-diam plunged holes ( $R_p/D = 0.375$ ) set at a spacing/hole diameter ratio of 2.75. For the purposes of identification these holes and their associated jets are numbered 1–16 in an anticlockwise direction when viewed from the base of the rig. An annular wedge is located on the inner wall of the feed annulus adjacent to the dilution holes and is designed to reduce the passage height from 35.8 to 10.4 mm. In this way, the rise in pressure across the face of the holes due to diffusion is reduced and the flow instabilities described by Lefebvre<sup>11</sup> minimized. No attempt is made to simulate the flow of air used for flame tube and turbine blade cooling that normally passes down the annulus between the liner and the combustor casing.

The outer casing of the rig is comprised of three sections, the lower one forming part of the settling length, the center housing the instrumentation, and the upper an entry length necessary to insure the required boundary-layer thickness in the crossflow prior to the dilution holes. The instrumentation section contains static pressure taps, mountings for five-hole pressure probes, and 16 thermocouples equispaced at 22.5-deg intervals, which can be located at any radial position in the crossflow annulus. Whereas the center tube is mounted on a fixed pedestal, the inner and the outer casing with the instru-

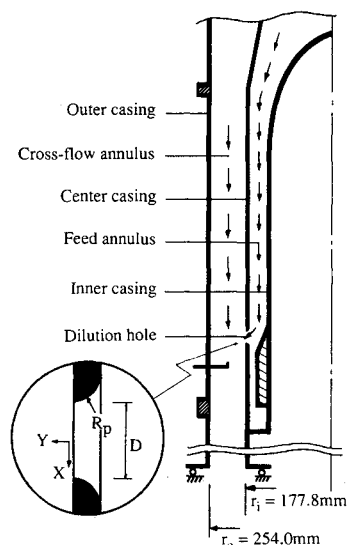


Fig. 2 Test facility.

mentation can be rotated to allow complete circumferential traversing. Two wooden spacer rings of 25.4- and 50.8-mm height provide the means for varying the vertical position of the instrumentation plane; thus, traverses can be made normal to the crossflow at distances of 1, 2, 3, and 4 dilution hole diameters downstream of the center of the hole.

Apart from temperature measurements, five-hole miniature pressure probes were traversed normal to the crossflow at  $X/D = 2.0$ . The probes, which provided flow angles as well as velocities, consisted of a cluster of five tubes 0.25-mm bore, 1.73-mm overall diameter and were used in the nonnull mode using the calibration procedure outlined by Wray.<sup>12</sup> In addition, surveys were made over the face of several jets at a nominal position of  $Y/D = 0.05$  from the exit plane of the dilution holes. The exact traverse plane location varied slightly about this nominal value because of expansion of the center casing with respect to the probe tip during operation of the test facility.

The 16 chromel/alumel thermocouples in the dilution zone together with thermocouples in the crossflow and the feed annuli were connected to a DEC LSI 11/23 microcomputer via two 10-channel Comark digital thermometers. Using 16 thermocouples, the entire flow in the circumferential direction could then be mapped by simultaneously traversing each thermocouple over a spacing equal to 2.75 hole diameters. Each time the temperatures were surveyed the 16 thermocouples were located at the same position relative to each dilution hole so that any recorded asymmetry was logged at the same flow condition. For a more detailed analysis of dilution zone mixing characteristics, a second series of tests was undertaken at  $X/D = 2.0$  involving measurements of temperature and pressure of certain jets at spacing intervals of  $S/45$  and 20 radial locations. In these tests temperature measurements were restricted to two jets while five-hole probe measurements were limited to a single jet per run. Data was also recorded at the exit plane of these dilution holes using a single probe traversed at increments  $D/16.4$  in both the lateral and axial directions. All of the data presented are based on measurements time-averaged over a period of 5 s prior to being committed to the memory of the microcomputer.

Corrections for minor variations in rig operating temperatures were made on the basis that at a fixed momentum flux ratio the nondimensional temperature  $\theta$  remains constant at a given location. Results are presented as values of  $\theta$  or corrected temperature  $T$  for reference conditions of  $T_j = 55^\circ\text{C}$  and  $T_c = 11^\circ\text{C}$ .

All pressure readings are corrected to a reference jet dynamic head of 50-mm water gauge, and the data derived from five-hole probe measurements are presented in terms of velocity distributions. Resolved components of velocity in the traversing plane are presented in the form of vectors, where the flow direction and magnitude of velocity at points in the plane are indicated by the direction and length of the arrows. Contours of constant velocity are used to indicate the magnitude of the velocity components perpendicular to the traverse plane.

### Mixing Parameters

The measured temperature distributions are presented in nondimensional form as

$$\theta = \frac{T - T_c}{T_j - T_c} \quad (1)$$

The preceding parameter may also be used to define the temperature distribution factors (TDF):

$$\text{mean TDF} = \frac{\bar{T}_r - T_c}{T_j - T_c} \quad (2)$$

where  $\bar{T}_r$  is the area-weighted mean temperature at a given

radius,

$$\text{maximum TDF} = \frac{\bar{T}_r - T_c}{T_j - T_c} \quad (3)$$

where  $\bar{T}_r$  is the maximum temperature at a given radius.

As a means of assessing the circumferential regularity of the flow the concept of a block distribution is introduced,<sup>10</sup> the physical size of which corresponds to the minimum geometric sector repeated around the annulus. In the case of these experiments, the 16 dilution holes mean that each jet is located within a 22.5-deg segment of the annulus, and for each traverse position a block temperature  $T_b$  is obtained by averaging the temperature measured in each sector at the same position relative to each dilution hole. By calculating block values at each traverse location a temperature distribution can be obtained that represents the mean sector temperature pattern around the annulus. Using the concept of a block, a further temperature distribution factor can be introduced:

$$\text{block maximum TDF} = \frac{(\bar{T}_b)_r - T_c}{T_j - T_c} \quad (4)$$

where  $(\bar{T}_b)_r$  is the maximum block temperature at a given radius.

The difference between the block maximum and mean temperature distributions indicates the degree of mixing between the jets and the crossflow. Since the maximum block  $(\bar{T}_b)_r$  and measured  $\bar{T}_r$  temperatures at a given radius can occur at any circumferential location, it should be noted that the maximum TDF parameters do not represent physical profiles.

Deviations in temperature of a given sector from that of the block distribution reflect circumferential asymmetries in the flowfield. The effect of such asymmetries is to increase the maximum temperature at any given radius, thereby influencing the turbine entry temperature profile. The difference between the highest temperature recorded at a given radius and the maximum block value at the same radius is therefore used to evaluate the asymmetry:

$$\text{temperature asymmetry factor (TAF)} = \frac{\bar{T}_r - (\bar{T}_b)_r}{T_j - T_c} \quad (5)$$

A jet asymmetry parameter  $\gamma$  can be defined to quantify the degree to which the temperature contours "twist" or rotate about the hole centerline ( $Z/D = 0$ ). The angles subtended by the lateral edges of the jet core (defined by the contours of high temperature) with respect to the hole centerline indicate the relative concentration of core fluid on either side of jet. Differences in the angles are used to denote the twist, a positive value of  $\gamma$  indicating a higher concentration of jet fluid to the left of the centerline.

## Results and Discussion

### Calibration Tests

To establish the circumferential uniformity of flow approaching the dilution holes in both the crossflow and the feed

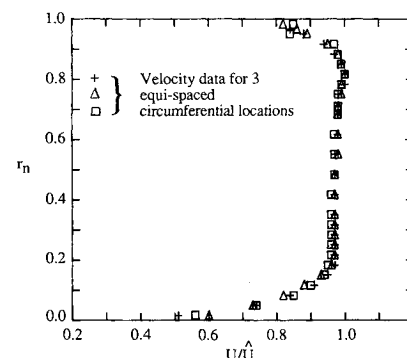


Fig. 3 Crossflow annulus velocity profiles.

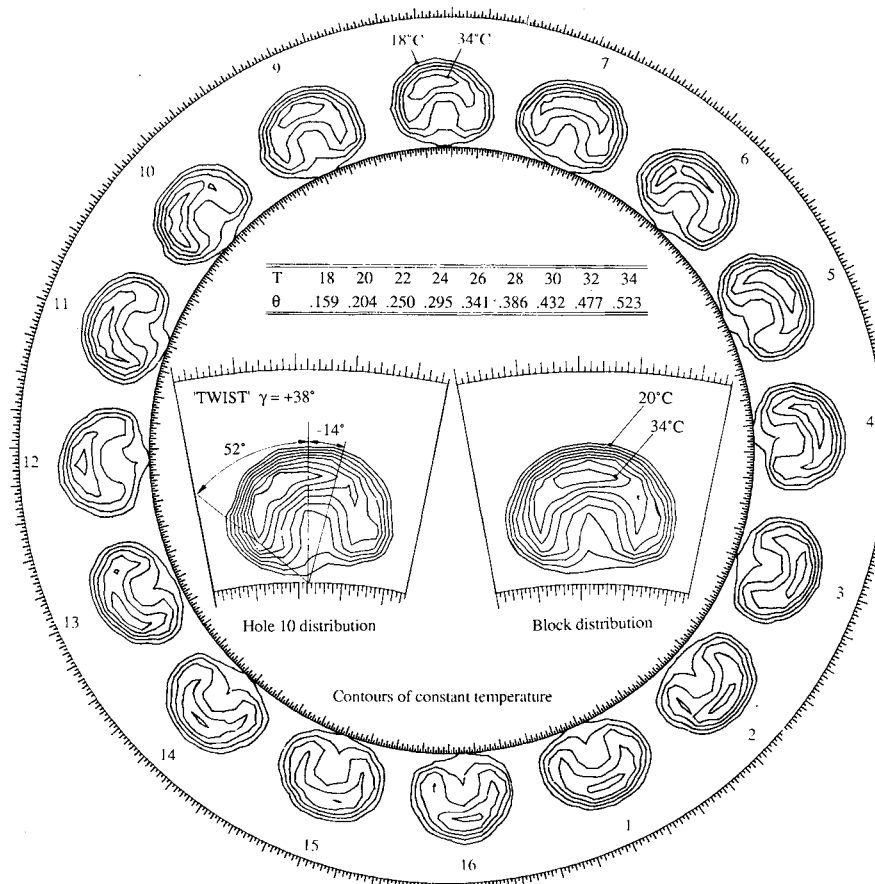


Fig. 4 Temperature distribution for holes 1-16 ( $X/D = 2.0$ ).

annuli, pressure surveys were carried out using pitot probes and wall static pressure taps. In assessing the symmetry of the crossflow no dilution air was supplied to the feed annulus, and in this way the performance of the intake and crossflow passage was established in the absence of any jet/crossflow interaction. The radial velocity profiles measured at three equispaced circumferential locations a distance of  $6D$  upstream of the dilution holes are shown in Fig. 3 where it will be seen that they are in excellent agreement. Information on the flow in the feed annulus was provided by a single rake containing five pitot probes mounted at  $X/D = 3.5$  on the inner casing, which could be rotated through  $360^\circ$ . Again, jet/crossflow interactions were avoided, in this case by blanking off the flare feeding the crossflow annulus. At a given radial location circumferential variations in velocity up to a maximum of 5% were observed, indicating good uniformity in the flow feeding the dilution holes.

#### Temperature Measurements

Having established the quality of the flow approaching the dilution holes, the temperature distribution at a distance  $X/D = 2.0$  was recorded using all 16 thermocouples. Contours of constant corrected temperature downstream of all 16 dilution holes together with the block temperature distribution are shown in Fig. 4, where it can be seen that each jet exhibits the characteristic kidney-shaped profile reported by many workers. However, despite the uniformity of the approaching flow circumferential asymmetries are observed, and Fig. 5a shows the radial variation of maximum temperature compared with the average and maximum block values. Figure 5b presents the radial variation of temperature on the axial centerline for the block distribution and the temperature asymmetry factor (TAF) from which it is seen that the largest asymmetry occurs at a nondimensional radius of 0.33 and is associated with a rotation or apparent twist of certain jets, which displaces relatively hot jet fluid to a lower radius than would otherwise be the case. Although the majority of the jets twist to some

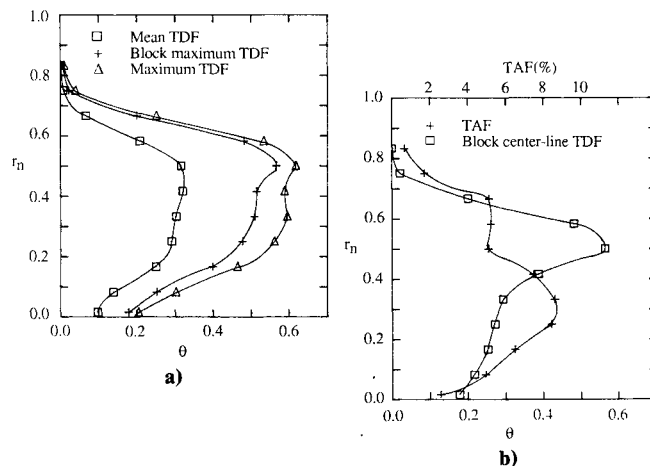


Fig. 5 Radial variation of temperature factors.

degree, the maximum asymmetry is associated with the jet issuing from hole 10, which exhibits a twist of  $38^\circ$ , and further testing confirmed the repeatability of this result. Investigation of the  $360^\circ$  temperature distribution is useful in establishing the overall lack of symmetry, but because of the restrictions imposed by rig running, time, and microcomputer storage, the data presented in Fig. 4 were obtained from a relatively coarse grid of data points, the radial and circumferential increments being 6.35 mm and  $2.5^\circ$ , respectively.

In order to obtain more detailed data on the behavior of certain jets, particularly those that exhibit a high degree of twist, measurements were made using a finer grid in the segment containing holes 7-12. The results obtained using this technique are presented in Fig. 6, and it will be observed that they are similar to those obtained previously. The jet issuing from hole 10 exhibits the highest twist, the effect of which can be seen in Fig. 7, which compares the radial variation of

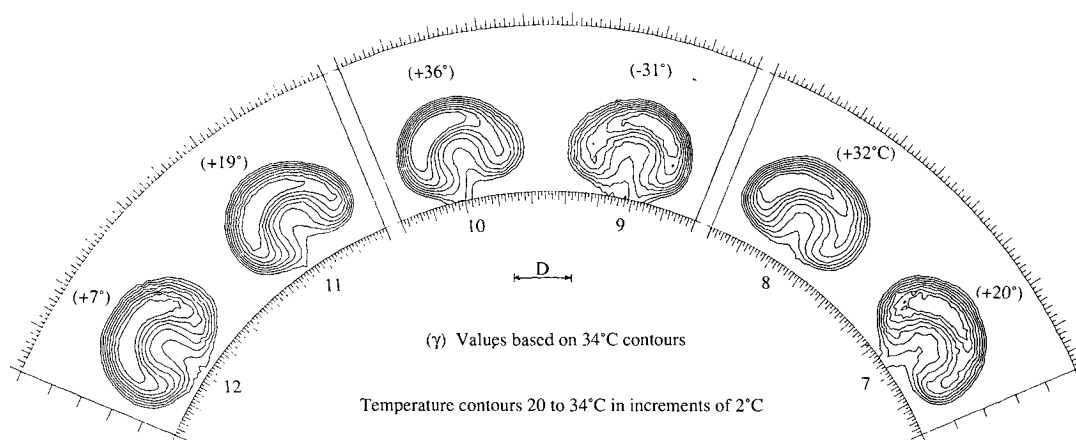


Fig. 6 Temperature distribution for holes 7-12 ( $X/D = 2.0$ ).

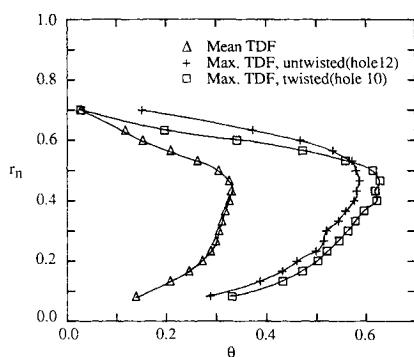


Fig. 7 Radial variation of maximum temperature in a twisted and untwisted jet.

maximum temperature in a twisted and untwisted jet (holes 10 and 12, respectively).

#### Flow at Exit of Dilution Holes

One possible explanation for the shape of the the constant-temperature contours is that a rotational component is present in certain jets as they discharge from the dilution holes. To test this theory, traverses were carried out using a miniature five-hole pressure probe across the exit plane of these dilution holes at  $Y/D = 0.05$ . Initially, tests were carried out in the absence of the crossflow with the outer casing removed, and under these conditions Fig. 8 shows that vortex structures are present in the rear half of certain dilution holes. For example, in the case of hole 9 a well-defined vortex with a clockwise sense of rotation is positioned to the left of the hole centerline, whereas a vortex with an opposite sense of rotation is similarly displaced but to the right of the centerline of hole 10. Tests indicate that this pattern of vortices in adjacent holes rotating in opposing directions continues around the annulus until interrupted by the pattern depicted in hole 8. Here the flow at the rear of the hole is symmetrical about the centerline with a component in an opposite sense to the direction of flow feeding the hole, either side of which are located two smaller vortices. It will be observed that due to the way in which air is fed to the holes along an approach annulus, even in the absence of the crossflow the jets exhibit a pronounced pitch component. To indicate the distribution of velocity components normal to the injection plane, contours of constant radial velocity for holes 8 and 10 have also been included in Fig. 8.

The way in which the velocity distribution in each hole is affected by the introduction of the crossflow is depicted in Fig. 9. The well-defined vortices in holes 9 and 10 are still present, but in the rear half of holes 7 and 8 asymmetry has

been produced with vortices of anticlockwise rotation being sited to the left of the hole centerlines. A summary of these effects for holes 8 and 10 is given in Fig. 10 in terms of the variation in pitch angle  $\alpha$  both along the axial centerline ( $Z/D = 0$ ) and the mean value over the face of the jet at a given axial location. Deflection of the jet by the crossflow is indicated by the increase in pitch angle, which is particularly evident in the front half of holes 8 and 10, where the angle increases by about 12 and 10 deg, respectively. Whereas the values along the centerline in the rear section of the hole are determined essentially by the position of the vortex, the mean values do indicate a reduction in pitch angle with the flow leaving almost normal to the surface. The radial velocity contours in Fig. 9 show how the flow in the jet is distorted by the crossflow even at a distance of  $Y/D = 0.05$ . For both holes the front half of the jet has a decreased velocity, and the flow in the rear half is forced to accelerate to accommodate the extra mass flow, which is in agreement with the findings of Crabb et al.<sup>13</sup> Furthermore, Fig. 9 indicates that in the rear half of the jet the crossflow causes a widening of the high-velocity region and, hence, the lateral stretching of the jet commences as it is formed.

#### Downstream Velocity Flowfield

Having established that vortices are formed in the jets as they issue from the dilution holes, the next phase of the test program was aimed at determining to what extent these vortices influenced the downstream structure of the flow. To this end, traverses were carried out normal to the wall using a miniature five-hole pressure probe at a distance downstream of two hole diameters in the segment containing holes 7-12. One of the difficulties in using such a probe is that large flow angles may be encountered particularly in the wake region, where flow recirculations are present. The probe calibration was only valid up to  $\pm 35$  deg in pitch and yaw, and so areas where data points are omitted indicate regions in which the flow angles are in excess of this value. Nonetheless, in certain areas where only one flow angle is outside the calibration limits an indication of the flow direction in one plane may be given, and where this has been done the data are represented by a dotted line.

As a single jet progresses downstream, Crabb et al.<sup>13</sup> and Kamotani and Greber<sup>14</sup> have shown that the core vortices control the mixing and location of jet fluid in the crossflow. For closely spaced multiple jets, however, the mechanism is more complex because of the interaction between the crossflow and core vortices. This is illustrated in Fig. 11 by vector plots of the velocities in the plane normal to the axial direction for holes 8, 9, and 10 with the contours of axial velocity being presented in Fig. 12. It will be seen that the crossflow accelerates into the spaces between the jets because of the action of the core vortices, is forced down toward the inner

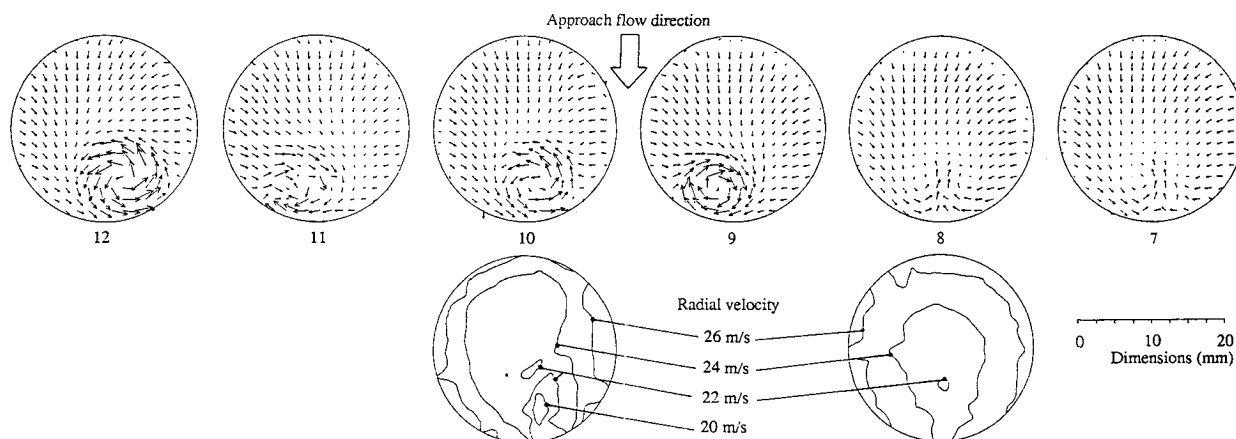


Fig. 8 Velocity distribution across the exit planes of holes 7-12 ( $Y/D = 0.05$ ) without crossflow.

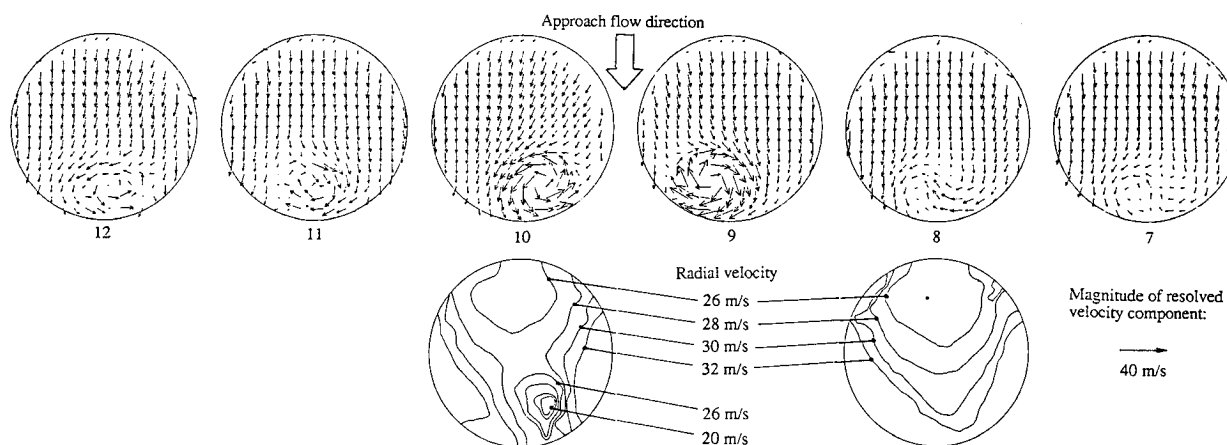


Fig. 9 Velocity distribution across the exit planes of holes 7-12 ( $Y/D = 0.05$ ) with crossflow.

wall. Part of this inflow passes downstream while the remainder is drawn into the low-pressure region at the rear of the jet, where it is opposed by flow coming from the other side and is forced upward away from the wall to form the crossflow vortices. The double-vortex structure reported by many workers investigating a single jet is clearly evident, but for the case of multiple jets the flowfield is more complex, with core vortices located at the lobes merging with the more dominant crossflow vortices. The stretching of the jet as it issues into the crossflow is presumably responsible for the rapid decay of the vortices formed in the dilution holes since their presence is not apparent at this location. What is clear, however, is that the double-vortex structure, which controls the mixing and location of jet fluid, is the principal feature of the flowfield.

The center-plane distribution of block temperature and axial velocity for holes 7-12 is presented in Fig. 13, the data being nondimensionalized with respect to the maximum values recorded. The location of the point of maximum velocity is seen to be at a greater radius than that of the jet (high-temperature) fluid, confirming the results of Crabb et al.<sup>13</sup> and Kamotani and Greber.<sup>14</sup> This effect is due to the entrainment of jet fluid into its own wake by the action of the double vortex and the acceleration of the crossflow, which is forced to pass over the obstruction caused by the jet.

An important feature apparent in Fig. 11 is that the double-vortex structure associated with most of the jets is asymmetric with the vortices, being of unequal strength. Furthermore, with the possible exception of hole 12, a correlation exists between the distortion or twisting of the temperature contours and the vortex structures, since the side of the jet with the highest concentration of jet (high-temperature) fluid corresponds to the location of the vortex of greatest strength. Since the behavior of the jet is controlled mainly by pressure forces that cause the bending of the jet and the formation of the

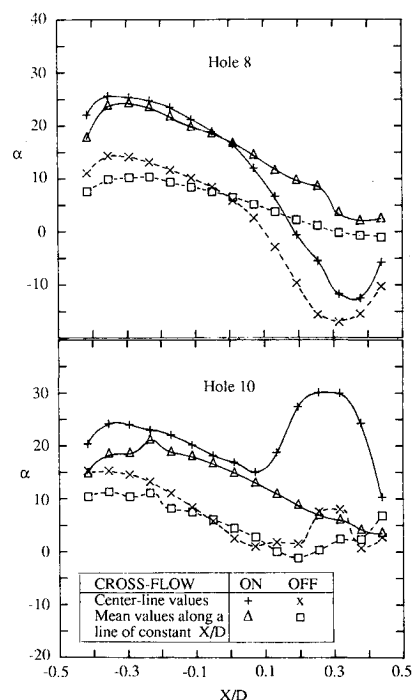


Fig. 10 Pitch angle variation along hole axis.

double-vortex structure, the subsequent shape of the jet must be dependent on the initial momentum distribution in the fluid issuing from the dilution hole. It has already been shown in

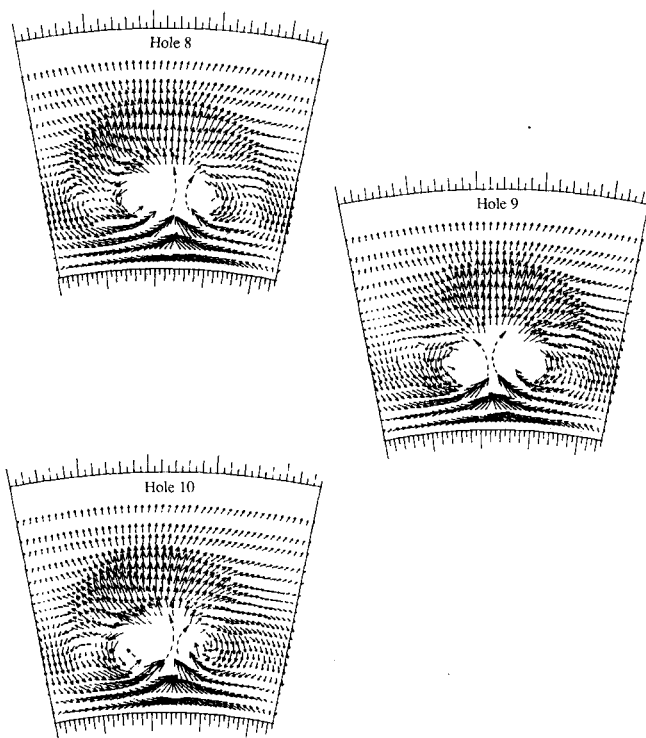


Fig. 11 Velocity vectors for holes 8-10 ( $X/D = 2.0$ ).

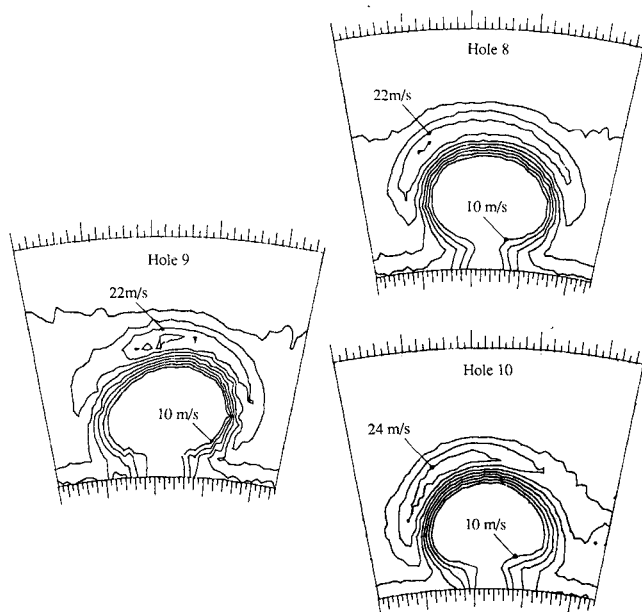


Fig. 12 Axial velocity distributions for holes 8-10 ( $X/D = 2.0$ ).

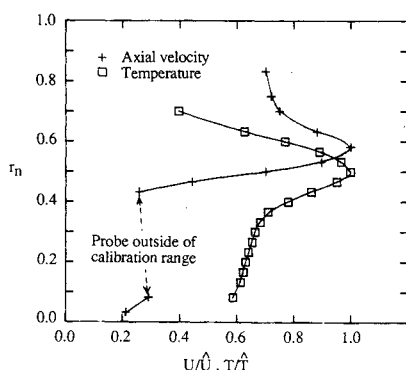


Fig. 13 Radial variation of enter-plane block temperature and axial velocities.

Fig. 9 that the velocity in the front half of the jet is reduced and that the momentum distribution is nonuniform. Lefebvre<sup>11</sup> has drawn attention to such effects and to the influence of backflow in the feed annulus on the formation of vortices in the holes and the attendant nonuniformities. It is therefore reasonable to assume that such nonuniformities could, under the action of pressure forces, lead to a nonuniform distribution of the jet fluid about the centerplane of the hole and be instrumental in the formation of vortices of unequal strength.

The contours of constant axial velocity downstream of holes 8-10 have been shown in Fig. 12. It is interesting to note that whereas the distribution for holes 9 and 10 supports the finding that the core of the jet has twisted, in the case of hole 8 the contours are almost symmetric and do not reflect the twist exhibited by the temperature contours. Although Fig. 9 indicates that the initial velocity distribution in hole 8 is more uniform than that in holes 9 and 10, the mechanism that determines the twist of the jets is considered to be the result of the combined influence of several factors. This is the subject of further investigation, but it is quite clear that the mechanisms at work are more complicated than those so far reported for a single jet, with a plenum feed, exhausting into a cross-flow.

### Conclusions

An experimental investigation has been carried out to study circumferential asymmetries in the flowfield downstream of a row of heated jets injected normally into a confined annular crossflow. The following conclusions are drawn:

- 1) An apparent twist or rotation of the temperature contours associated with certain jets is responsible for the circumferential asymmetry of the temperature distribution.
- 2) The double-vortex structure, which is the dominant feature of the downstream flowfield, is usually composed of vortices of unequal strength.
- 3) The side of the jet with the highest concentration of high-temperature jet fluid corresponds to the location of the vortex of greatest strength.
- 4) Multiple jets fed from an annular approach passage and discharging from plunged circular holes exhibit across their exit planes nonuniformities in both flow direction and distribution. The flow in the front of the hole is reduced, and vortices are formed in the rear half. These effects are accentuated in the presence of a crossflow.

The way in which the nonuniformities in the flow issuing from the holes influence the structure of the downstream flowfield is the subject of a continuing investigation.

### Acknowledgments

This work was supported by The Ministry of Defence, Royal Aircraft Establishment, Pyestock, Farnborough, Contract ER/2170/090 XR. The authors wish to express their appreciation to Messrs. G. Hodson, R. Marson, and D. Glover for their assistance in the design and construction of the test rig and to Miss S. Armitage for her help in running the facility.

### References

- <sup>1</sup>Norgren, C. T. and Humanik, F. M., "Dilution-Jet Mixing Study for Gas-Turbine Combustors," NASA TN D-4695, 1968.
- <sup>2</sup>Sridhara, K., "Gas Mixing in the Dilution Zone of a Combustion Chamber," National Aeronautical Laboratory, TN 30, 1970.
- <sup>3</sup>Kamotani, Y. and Greber, J., "Experiments on Confined Turbulent Jets in Cross-Flow," NASA CR-2392, 1974.
- <sup>4</sup>Holdeman, J. D., Walker, R. E., and Kors, D. L., "Mixing of a Row of Jets with a Confined Crossflow," *AIAA Journal*, Vol. 15, Feb. 1977, pp. 243-249; see also NASA TM X-71426.
- <sup>5</sup>Crabb, D. and Whitelaw, J. H., "The Influence of Geometric

Asymmetry on the Flow Downstream of a Row of Jets Discharging Normally into a Freestream," *Journal of Heat Transfer*, Vol. 101, Feb. 1979, p. 183.

<sup>6</sup>Witig, S. L. K., Elbahar, D. M. F., and Noll, B. E., "Temperature Profile Development in Turbulent Mixing of Coolant Jets with a Confined Hot Cross-Flow," *Journal of Engineering for Gas Turbines and Power*, Vol. 106, Jan. 1984, p. 193.

<sup>7</sup>Holdeman, J. D., Srinivasan, R., and Berenfield, A., "Experiments in Dilution Jet Mixing," *AIAA Journal*, Vol. 22, Oct. 1984, pp. 1436-1443; see also NASA CR-168031 and NASA CR-174624.

<sup>8</sup>Holdeman, J. D. and Srinivasan, R., "Modeling Dilution Jet Flowfields," *Journal of Propulsion and Power*, Vol. 2, Jan.-Feb. 1986, pp. 4-10; see also NASA-CR-175043, 1986.

<sup>9</sup>Holdeman, J. D., Srinivasan, R., Coleman, E. B., Meyers, G. D., and White, C. D., "Effects of Multiple Rows and Noncircular Ori-

fices on Dilution Jet Mixing," *Journal of Propulsion and Power*, Vol. 3, May-June 1987, pp. 219-226; see also NASA TM-86996.

<sup>10</sup>Shaw, D., Rolls Royce Internal Rept. PD2181.

<sup>11</sup>Lefebvre, A. H., *Gas Turbine Combustion*, McGraw-Hill, New York, 1983.

<sup>12</sup>Wray, A. P., "The Use of a 5-Hole Probe as a Non-Nulled Instrument and the Analysis of Test Data Using the Computer Programs 5HP1, 5HP2 and 5HP3," TT86R02, Dept. of Transport Technology, University of Technology, Loughborough, UK, TT86R02, Jan. 1986.

<sup>13</sup>Crabb, D., Durao, D. F. G., and Whitelaw, J. H., "A Round Jet Normal to a Cross-Flow," *Journal of Fluids Engineering*, Vol. 103, March 1981, pp. 142-152.

<sup>14</sup>Kamotani, Y. and Greber, I., "Experiments on a Turbulent Jet in a Cross-Flow," *AIAA Journal*, Vol. 10, Nov. 1972.

## Recommended Reading from the AIAA

Progress in Astronautics and Aeronautics Series . . . 

# Opportunities for Academic Research in a Low-Gravity Environment

George A. Hazelrigg and Joseph M. Reynolds, editors

The space environment provides unique characteristics for the conduct of scientific and engineering research. This text covers research in low-gravity environments and in vacuum down to  $10^{-15}$  Torr; high resolution measurements of critical phenomena such as the lambda transition in helium; tests for the equivalence principle between gravitational and inertial mass; techniques for growing crystals in space—melt, float-zone, solution, and vapor growth—such as electro-optical and biological (protein) crystals; metals and alloys in low gravity; levitation methods and containerless processing in low gravity, including flame propagation and extinction, radiative ignition, and heterogeneous processing in auto-ignition; and the disciplines of fluid dynamics, over a wide range of topics—transport phenomena, large-scale fluid dynamic modeling, and surface-tension phenomena. Addressed mainly to research engineers and applied scientists, the book advances new ideas for scientific research, and it reviews facilities and current tests.

**TO ORDER: Write, Phone, or FAX:** AIAA c/o TASC0,  
9 Jay Gould Ct., P.O. Box 753, Waldorf, MD 20604  
Phone (301) 645-5643, Dept. 415 ■ FAX (301) 843-0159

Sales Tax: CA residents, 7%; DC, 6%. For shipping and handling add \$4.75 for 1-4 books (call for rates for higher quantities). Orders under \$50.00 must be prepaid. Foreign orders must be prepaid. Please allow 4 weeks for delivery. Prices are subject to change without notice. Returns will be accepted within 15 days.

**1986 340 pp., illus. Hardback**  
**ISBN 0-930403-18-5**  
**AIAA Members \$59.95**  
**Nonmembers \$84.95**  
**Order Number V-108**